Viscoelastic behaviour of glass beads reinforced poly(butylene terephthalate): experimental and theoretical approaches

O. Beaudoin, Anne Bergeret, Jean-christophe Quantin, A. Crespy

Viscoelastic behaviour of glass beads reinforced poly(butylene terephthalate): experimental and theoretical approaches

O. BEAUDOIN, A. BERGERET*, J.-C. QUANTIN and A. CRESPY

Ecole des Mines d'Alès, Laboratoire Matrices, Matériaux Minéraux et Organiques, 6 avenue de Clavières, 30319 Alès Cedex, France

Abstract—The dynamic mechanical behaviour of a series of poly(butylene terephthalate)/ glass beads composites was studied as a function of filler ratio, filler size and surface treatment. Samples were subjected to compression–tension testing within a temperature range from −150°C to 150°C. The real part (E') of the dynamic modulus and the loss tangent ($\tan\delta$) were studied around β and α relaxations. It was observed that the magnitude of these relaxations decreased as the glass beads ratio increased. A similar decrease was observed at constant filler ratio with improving filler–matrix adhesion by a coupling agent. All these results might be due both to the matrix substitution by fillers and to the reducing of polymer chains molecular mobility in the vicinity of the interface. Using Hashin's correspondence principle, the viscoelastic behaviour of such composites was described by self-consistent models in the neighbourhood of the α relaxation and compared to experimental data.

Keywords: Glass beads; poly(butylene terephthalate); interphase; viscoelastic behaviour; molecular mobility; Poisson's ratio; self-consistent models.

1. INTRODUCTION

Mechanical properties of composites reinforced by mineral fillers depends not only on the properties of each constituent, but also on the filler shape and the nature of bonds between particles and matrix [1–4] since the load transfer occurs at the interface or in the interphase between the two phases.

Among experimental techniques for the study of interfacial phenomena [5–9], dynamic mechanical spectrometry is particularly interesting, especially in the case of heterogeneous and isotropic composites such as a polymer matrix reinforced by spherical particles. Up to now, the amplitude of mechanical relaxation attributed to

*To whom correspondence should be addressed. E-mail: abergere@ensm-ales.fr

the glass transition of the polymer matrix depends to a large extent on microstructural characteristics (filler content, particulate size distribution and surface treatment) [9, 10].

The purpose of this work is: (a) to analyze the influence of these microstructural parameters on the viscoelastic behaviour of several composites; (b) to simulate the viscoelastic behaviour through self-consistent models developed in linear viscoelasticity according to Hashin's correspondence principle [11] and compare theoretical data to experimental results.

2. EXPERIMENTAL

2.1. Materials

The polymer used in this study was a semicrystalline thermoplastic polyester (poly(butylene terephthalate) (PBT)) provided by Dupont de Nemours Company.

Glass beads were supplied by Sovitec Company in different size distributions and different surface treatments by silane coupling agents. The weight fraction of coating on glass beads is estimated at about 0.1% (Table 1).

The inclusions have an elastic behaviour with a Young's modulus of 70 GPa and a Poisson's ratio of 0.2.

2.2. Sample preparation

Composite specimens were PBT reinforced by 15 and 40 wt% of glass beads and were elaborated through an extrusion process and an injection molding.

Composite materials were first prepared by mixing the polymer matrix and the glass beads in a twin-screw extruder at 270°C. Then, the pellets of compound were injection molded at 270°C and cooled in the mould at 80°C. Thus, the effective filler fractions, as reported in Table 2, were measured by burning the samples at 625°C for 4 h according to the international ISO 1172 standard.

Table 1.
Characteristics of glass beads

Average diameter (μm)	Surface treatment	Fraction of coating (wt%)
20	untreated (UT)	
20	vinylsilane (VS)	0.11 ± 0.01
20	aminosilane (AS)	0.13 ± 0.01
40	untreated (UT)	
40	vinylsilane (VS)	0.12 ± 0.01
40	aminosilane (AS)	0.10 ± 0.01
90	untreated (UT)	

2.3. *Experimental techniques*

Dynamic mechanical spectrometry was carried out using a viscoelasticimeter (Metravib Company) within a temperature range from −150 to 150°C under isochrone conditions (5 Hz). Parallelepipedic samples (25 × 4 × 2 mm) were cut from injection molded dumbbells using a diamond band saw and were subjected to compression–tension testing with a displacement of ±5 μm. The real part (E') of the dynamic modulus and the loss tangent ($\tan\delta$) were used.

3. EXPERIMENTAL

Several authors have studied the viscoelastic behaviour of composites reinforced by glass beads, but the corresponding host polymers were amorphous [9, 10]. The presence of crystalline units could induce complex relaxation phenomena. Previous studies on PET showed a decrease in the loss tangent $\tan\delta$ near both β and α transitions with increasing crystallinity [12, 13]. Therefore, this parameter must be measured on samples before dynamic mechanical tests.

The crystallinity of all samples was studied through melt enthalpy measurement by using a Differential Scanning Calorimeter (DSC 92 Setaram). Typical sample weight used for experiments was 20 mg. Scans were carried out with a heating rate of 20°C/min from room temperature to 300°C.

The results showed no influence of surface treatment on crystallinity (Table 2). Otherwise, crystallinity decreases with rise in either the filler content or the average diameter. These trends might be attributed to an increase of the matrix cooling rate induced by: (i) the matrix substitution by glass beads (thermal diffusivity being higher for glass than for melt polymer [4, 14, 15]); or (ii) the increase of distances between particles.

Moreover, no significant influence of the average size of fillers on the melting endotherms was observed.

Table 2.
Characteristics of poly(butylene terephthalate)/glass beads composites

Sample	Average diameter (μm)	Effective filler fraction (wt%)	Surface treatment	Melt enthalpy (J/g)
PBT				−51.6 ± 1.2
	20	14.5	untreated (UT)	−46.6 ± 1.5
2	20	39.1	untreated (UT)	−40.3 ± 1.7
3	20	41.7	vinylsilane (VS)	−43.3 ± 0.9
4	20	41.2	aminosilane (AS)	−42.9 ± 1.3
5	40	40.2	untreated (UT)	−43.4 ± 0.6
6	40	40.0	vinylsilane (VS)	−44.6 ± 1.5
7	40	38.8	aminosilane (AS)	−44.6 ± 1.0
8	90	39.9	untreated (UT)	−52.7 ± 1.3

3.1. Influence of the glass beads ratio

Figure 1 shows the real part (E') of the dynamic modulus and the loss tangent ($\tan\delta$) curves recorded at 5 Hz for composites reinforced by 15 and 40 wt% of untreated fillers (average diameter 20 μm) and for pure PBT. With increasing the glass beads content, the magnitudes of β and α mechanical relaxations are decreased. Similar variations were obtained with treated or untreated glass beads of different size distributions. Moreover, with increase of the filler ratio, the $\tan\delta$ maximum is slightly shifted towards lower temperatures, as shown in Table 3. This tendency was not always observed on the β relaxation, probably owing to multiple origins of relaxation process. Indeed, molecular motions connected to β relaxation in poly(methylene terephthalate) polymers such as PET or PBT, could be attributed to the superposition of two or three different relaxation processes due to the mobility of $-CH_2$ and 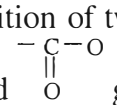 groups [13, 16].

All these results might be due both to the matrix substitution by fillers and to the reducing of polymer chains mobility in the vicinity of the interface. Furthermore, the real part (E') of the dynamic modulus increased at the same time.

In these composite samples, the crystallinity of the polymer matrix has an antagonist effect on the amplitude of β and α relaxations, which is negligible compared to the effect of the filler ratio.

3.2. Influence of the surface treatment

Figure 2 shows the real part (E') of the dynamic modulus and the loss tangent ($\tan\delta$) curves recorded at 5 Hz for composites reinforced by 40 wt% of glass beads (average diameter 20 μm). The nature of the glass beads coating seems to have an influence on the magnitude of α and β mechanical relaxations. These results might be attributed to the chemical links between the coupling agent and polymer chains. The stronger these links, the lower the magnitude of the mechanical relaxations.

In the case of a vinylsilane agent, weak links (van der Waals) between vinyl functions and 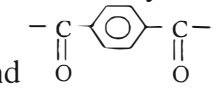 groups of PBT might be assumed.

For an aminosilane agent, covalent links between amine groups and end PBT chain functions (carboxylic or alcohol) or hydrogen links between hydrogen atoms of amine groups and oxygen atoms inside PBT chains, might be supposed.

Furthermore, the real part (E') of the dynamic modulus increases in the presence of a silane coating, especially aminosilane agent. On the other hand, no shift of the relaxations was observed. Otherwise, crystallinity of the polymer matrix was not taken into account, insofar as filler surface treatment is not a factor which could modify the crystalline structure, as seen earlier (Table 2).

2.3. *Experimental techniques*

Dynamic mechanical spectrometry was carried out using a viscoelasticimeter (Metravib Company) within a temperature range from −150 to 150°C under isochrone conditions (5 Hz). Parallelepipedic samples (25 × 4 × 2 mm) were cut from injection molded dumbbells using a diamond band saw and were subjected to compression–tension testing with a displacement of ±5 μm. The real part (E') of the dynamic modulus and the loss tangent ($\tan\delta$) were used.

3. EXPERIMENTAL

Several authors have studied the viscoelastic behaviour of composites reinforced by glass beads, but the corresponding host polymers were amorphous [9, 10]. The presence of crystalline units could induce complex relaxation phenomena. Previous studies on PET showed a decrease in the loss tangent $\tan\delta$ near both β and α transitions with increasing crystallinity [12, 13]. Therefore, this parameter must be measured on samples before dynamic mechanical tests.

The crystallinity of all samples was studied through melt enthalpy measurement by using a Differential Scanning Calorimeter (DSC 92 Setaram). Typical sample weight used for experiments was 20 mg. Scans were carried out with a heating rate of 20°C/min from room temperature to 300°C.

The results showed no influence of surface treatment on crystallinity (Table 2). Otherwise, crystallinity decreases with rise in either the filler content or the average diameter. These trends might be attributed to an increase of the matrix cooling rate induced by: (i) the matrix substitution by glass beads (thermal diffusivity being higher for glass than for melt polymer [4, 14, 15]); or (ii) the increase of distances between particles.

Moreover, no significant influence of the average size of fillers on the melting endotherms was observed.

Table 2.
Characteristics of poly(butylene terephthalate)/glass beads composites

Sample	Average diameter (μm)	Effective filler fraction (wt%)	Surface treatment	Melt enthalpy (J/g)
PBT				−51.6 ± 1.2
1	20	14.5	untreated (UT)	−46.6 ± 1.5
2	20	39.1	untreated (UT)	−40.3 ± 1.7
3	20	41.7	vinylsilane (VS)	−43.3 ± 0.9
4	20	41.2	aminosilane (AS)	−42.9 ± 1.3
5	40	40.2	untreated (UT)	−43.4 ± 0.6
6	40	40.0	vinylsilane (VS)	−44.6 ± 1.5
7	40	38.8	aminosilane (AS)	−44.6 ± 1.0
8	90	39.9	untreated (UT)	−52.7 ± 1.3

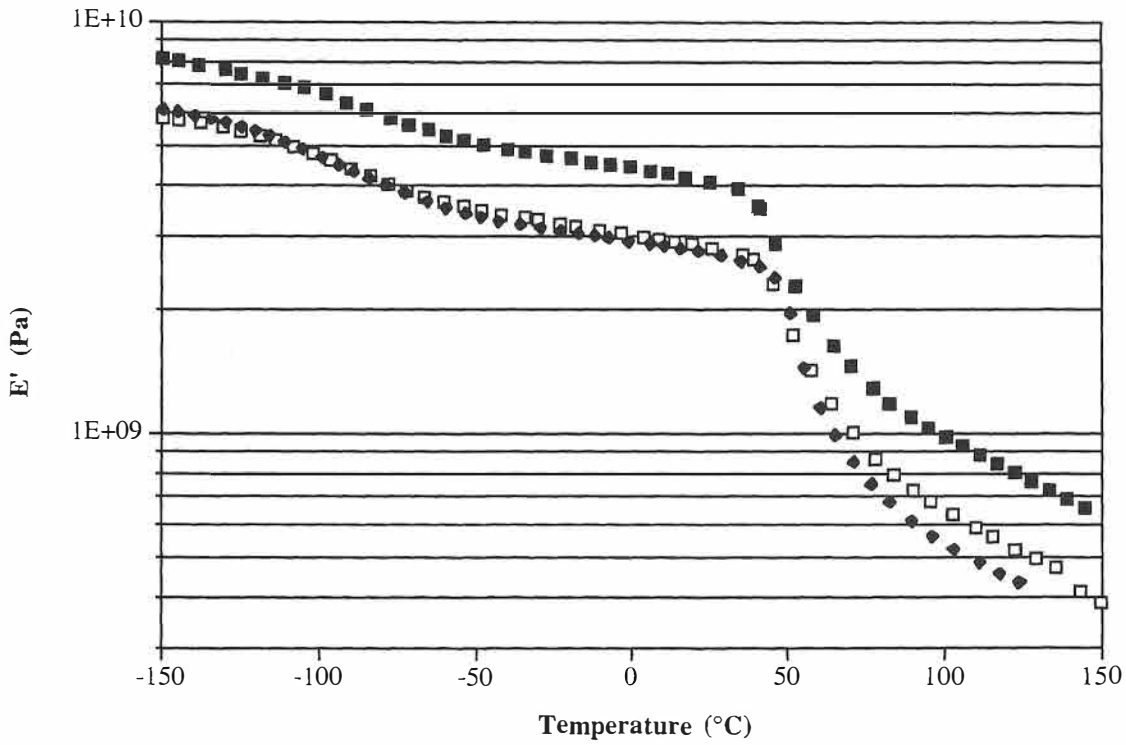

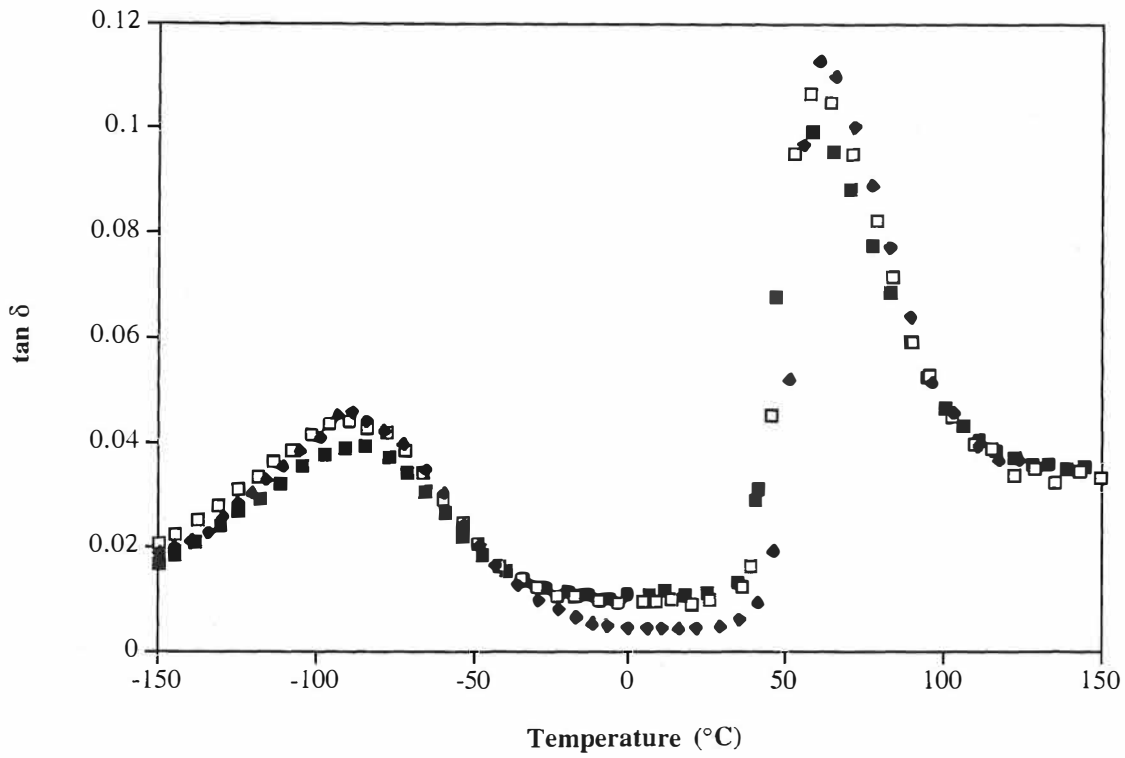

Figure 1. Curves of E' and $\tan\delta$ *versus* temperature at 5 Hz for (◆) a pure poly(butylene terephthalate) and reinforced by (□) 15 wt% and (■) 40 wt% of untreated glass beads.

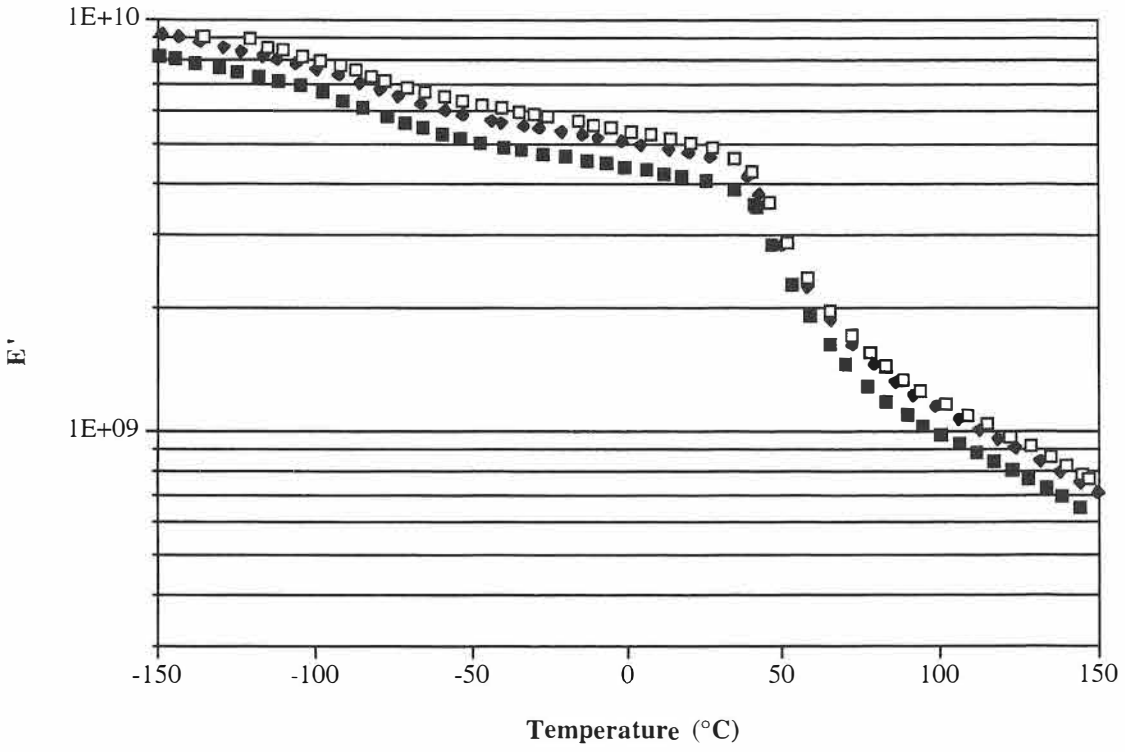

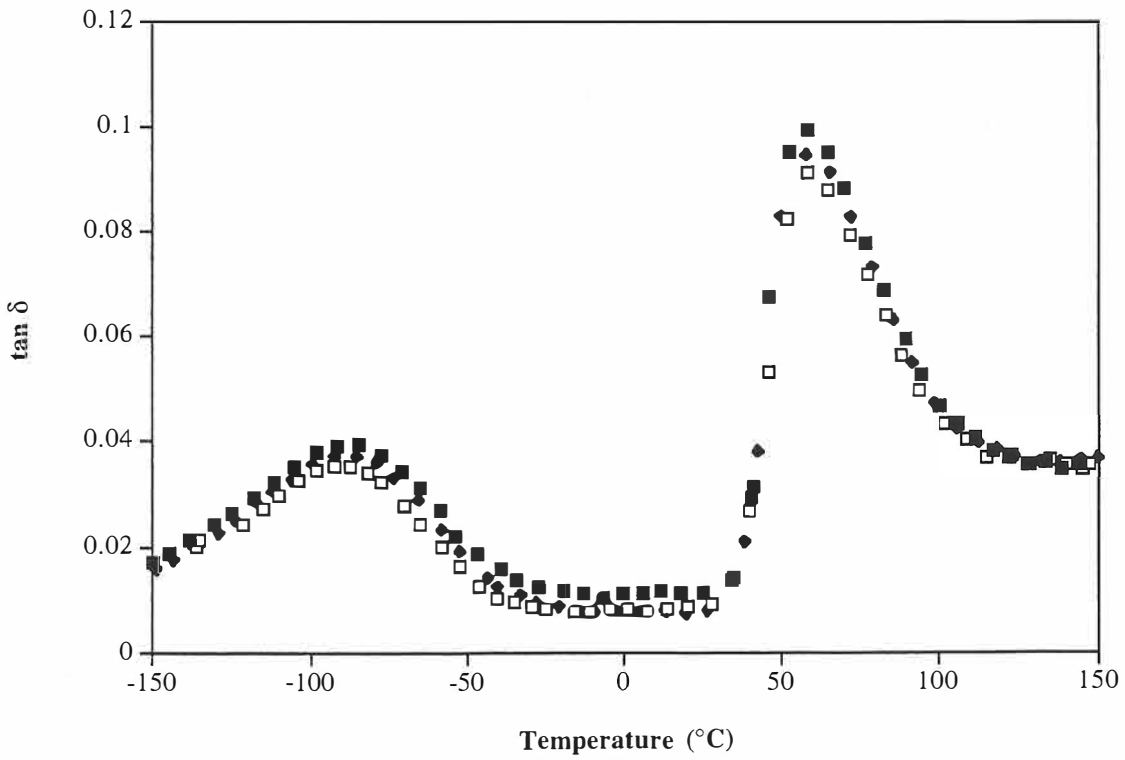

Figure 2. Curves of E' and $\tan\delta$ *versus* temperature at 5 Hz for a poly(butylene terephthalate) reinforced by 40 wt% of (■) untreated glass beads or coated by (◆) a vinylsilane and (□) an aminosilane coupling agent.

Table 3.
Results obtained for β and α mechanical relaxations in the case of poly(butylene terephthalate)/glass beads composites

Sample	T_β (°C)	tan δ_β	T_α (°C)	tan δ_α
PBT	-85.2 ± 0.4	0.044	61.4 ± 0.9	0.114
1	-89.9 ± 0.2	0.043	59.9 ± 0.1	0.107
2	-88.5 ± 1.3	0.040	58.7 ± 0.4	0.099
3	-87.8 ± 0.2	0.038	60.0 ± 0.4	0.094
4	-90.0 ± 0.9	0.036	59.0 ± 0.4	0.091
5	-84.5 ± 1.3	0.038	58.2 ± 0.6	0.096
6	-88.7 ± 0.9	0.038	59.3 ± 0.9	0.093
7	-84.8 ± 0.6	0.038	58.2 ± 0.1	0.093
8	-86.6 ± 0.5	0.039	60.0 ± 0.4	0.096

3.3. Influence of the particle size for a constant mass fraction of fillers

Any particular difference between the amplitude of β and α relaxations was observed in the range of size distribution studied. All these results are summarized in Table 3.

So, crystallinity of the matrix seems to have an influence on the viscoelastic behaviour of the composites. Nevertheless, sensitivity of this parameter on the characteristics of β and α mechanical relaxations should be studied from now on.

4. MECHANICAL PREDICTION

Among the various elastic models extended to the viscoelastic behaviour description of composites [17–23], self-consistent model approaches were chosen. These models are very interesting because they take into account the filler shape (spherical particles) and the Poisson's ratio of the polymer matrix [22, 23].

These approaches predict the composite complex modulus E_c^* through the determination of the complex bulk modulus K_c^* and the complex shear modulus G_c^*, in accordance with the following formula:

$$E^* = \frac{9G_c^* K_c^*}{G_c^* + 3K_c^*}. \tag{1}$$

4.1. Christensen and Lo's model

Christensen and Lo proposed a geometric model of the composite material, consisting of a single spherical filler coated by a layer of matrix and embedded in an infinite equivalent homogeneous medium, having effective properties of composite material [22] (Fig. 3).

If the specimen is subjected to a hydrostatic stress P on the outer boundary of this Representative Elementary Volume (R.E.V.) of the composite material, the bulk

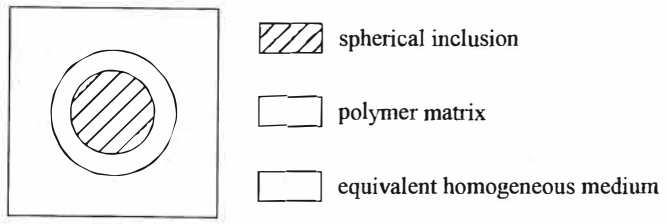

Figure 3. Christensen and Lo's self-consistent model.

modulus can be determined, assuming continuity conditions on displacement and traction stresses at the interfaces. Using Hashin's correspondence principle [11], the calculation of the effective bulk modulus K_c^* of the homogeneous sphere leads to the following relation, V_f being the volume fraction of inclusions:

$$K_c^* = K_m^* + \frac{V_f(K_f - K_m^*)}{1 + (1 - V_f)\dfrac{(K_f - K_m^*)}{K_m^* + \dfrac{4}{3}G_m^*}}, \tag{2}$$

with m, f and c indices for matrix, filler and composite, respectively.

For the determination of the effective shear modulus, Christensen and Lo assumed a general displacement for the R.E.V. in the form:

$$\begin{aligned} U_r &= U_r(r)\sin^2\theta\cos 2\psi, \\ U_\theta &= U_\theta(r)\sin\theta\cos\theta\cos 2\psi, \\ U_\psi &= U_\psi(r)\sin\theta\sin 2\psi, \end{aligned} \tag{3}$$

where $U_r(r)$, $U_\theta(r)$ and $U_\psi(r)$ are unknown functions of the radius r of the sphere, obtained from the equilibrium equations. Then, using Eshelby's approach [24] for a homogeneous medium containing an inclusion, strain energy under applied displacement conditions is determined in the R.E.V. and in the equivalent homogeneous medium. Assuming both the results to be equal, Christensen determined the complex shear modulus through a quadratic equation having only one available solution:

$$A\left(\frac{G_c^*}{G_m^*}\right)^2 + 2B\left(\frac{G_c^*}{G_m^*}\right) + C = 0, \tag{4}$$

with A, B, C coefficients which depend on characteristics of the matrix (E_m^*, ν_m^*), the glass beads (E_f, ν_f) and on the volume fraction of inclusions V_f.

The composite complex modulus is obtained from the relation (1).

4.2. Maurer's model

This approach is quite similar to Christensen and Lo's model but this model takes into account a fourth phase (interphase) between the spherical particle and the matrix coating [23], as shown in Fig. 4.

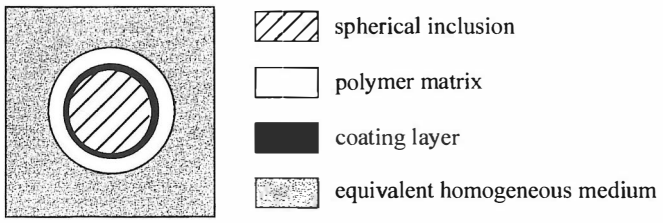

Figure 4. Maurer's self-consistent model.

If the composite is subjected to a hydrostatic stress P on the outer boundary of this R.E.V., the complex bulk modulus can be determined with the same assumptions used in the three-phase self-consistent model:

$$K_c^* = \frac{K_f V_f + K_i^* V_i R_k + K_m^* V_m S_k}{V_f + V_i R_k + V_m S_k}, \tag{5}$$

where:

$$R_k = \frac{3K_f + 4G_i^*}{3K_i^* + 4G_i^*},$$

$$S_k = \frac{(3K_f + 4G_i^*)(3K_i^* + 4G_m^*) - 12d(K_i^* - K_f)(G_i^* - G_m^*)}{(3K_m^* + 4G_m^*)(3K_i^* + 4G_i^*)},$$

$$d = \frac{V_f}{V_f + V_i}.$$

As regards the composite complex shear modulus G_c^*, Maurer obtained a quadratic equation similar to (4):

$$40|X|\left(\frac{G_c^*}{G_m^*}\right)^2 + \left(2|Y| + 8|Z|\right)\left(\frac{G_c^*}{G_m^*}\right) - 5|T| = 0, \tag{6}$$

where $|X|$, $|Y|$, $|Z|$ and $|T|$ are the determinants of 10×10 matrices. The elements of these matrices depend on characteristics of the matrix (E_m^*, ν_m^*), the coating layer (E_i^*, ν_i^*), the glass beads (E_f, ν_f) and on the volume fraction of inclusions and of the coating layer (V_f, V_i).

The composite complex modulus is obtained from relation (1).

4.3. Numerical results and discussion

The inclusions and matrix characteristics at room temperature are reported in the Experimental Materials section. The glass beads have an elastic behaviour over the analyzed temperature range around α relaxation (20–100°C). For the polymer matrix, a complex Poisson's ratio must be determined from the complex modulus experimentally measured. Ultrasonic measurements allow to determine also these values in the studied temperature range, but the experimental data are difficult to obtain [25, 26].

Some authors have developed prediction models. Kolsky [27] supposed the independence in time and temperature of the matrix bulk modulus:

$$K_{\mathrm{m}}^{*}(T) = K_{\mathrm{m}}^{*}(T_{\mathrm{o}}), \tag{7}$$

with:

$$K_{\mathrm{m}}^{*} = \frac{E_{\mathrm{m}}^{*}}{3(1 - 2\nu_{\mathrm{m}}^{*})}. \tag{8}$$

The relations (7) and (8) lead to the following result:

$$\nu_{\mathrm{m}}^{*}(T) = \frac{1}{2}\left[1 - \frac{E_{\mathrm{m}}^{*}(T)}{E_{\mathrm{m}}^{*}(T_{\mathrm{o}})}\right]\left(1 - 2\nu_{\mathrm{m}}^{*}(T_{\mathrm{o}})\right), \tag{9}$$

where $\nu_{\mathrm{m}}^{*}(T_{\mathrm{o}}) = 0.3$ (elastic value at room temperature).

On the other hand, Theocaris and Hadjijoseph [28] assumed a slight variation of the matrix bulk modulus and of the Poisson's ratio with the temperature, but not at each increment of temperature:

$\forall j \in [0, n]$ (j corresponding to temperature increment):

$$\nu_{\mathrm{m}}^{*}(T_{2j+1}) = \nu_{\mathrm{m}}^{*}(T_{2j}), \tag{10}$$

$$K_{\mathrm{m}}^{*}(T_{2j+2}) = K_{\mathrm{m}}^{*}(T_{2j+1}). \tag{11}$$

The relations (8) and (10) lead to the following expression:

$$K_{\mathrm{m}}^{*}(T_{2j+1}) = K_{\mathrm{m}}^{*}(T_{2j})\,\frac{E_{\mathrm{m}}^{*}(T_{2j+1})}{E_{\mathrm{m}}^{*}(T_{2j})}. \tag{12}$$

Otherwise, the relations (8) and (11) gave the relation:

$$\nu_{\mathrm{m}}^{*}(T_{2j+2}) = \frac{1}{2} - \frac{1}{E_{\mathrm{m}}^{*}(T_{2j+1})}\left(\frac{1}{2} - \nu_{\mathrm{m}}^{*}(T_{2j+1})\right)E_{\mathrm{m}}^{*}(T_{2j+2}). \tag{13}$$

Using elasticity laws, the prediction method can be completed by relations (14) and (15), as described below:

$$K_{\mathrm{m}}^{*}(T_{2j}) = \frac{E_{\mathrm{m}}^{*}(T_{2j})}{3\left(1 - 2\nu_{\mathrm{m}}^{*}(T_{2j})\right)}, \tag{14}$$

$$\nu_{\mathrm{m}}^{*}(T_{2j+1}) = \frac{1}{2} - \frac{E_{\mathrm{m}}^{*}(T_{2j+1})}{6K_{\mathrm{m}}^{*}(T_{2j+1})}. \tag{15}$$

Now, the complex Poisson's ratio and complex bulk modulus may be alternatively obtained by relations (14), (12), (15) and (13) from the real value at room temperature ($\nu_{\mathrm{m}} = 0.3$), as described in Fig. 5.

4.3.1. Determination of the complex Poisson's ratio of the polymer matrix — choice of the prediction method. The two previous simulations suggested for the determination of the complex Poisson's ratio of the polymer matrix were compared, as reported in Fig. 6. The comparison between these two approaches leads to similar

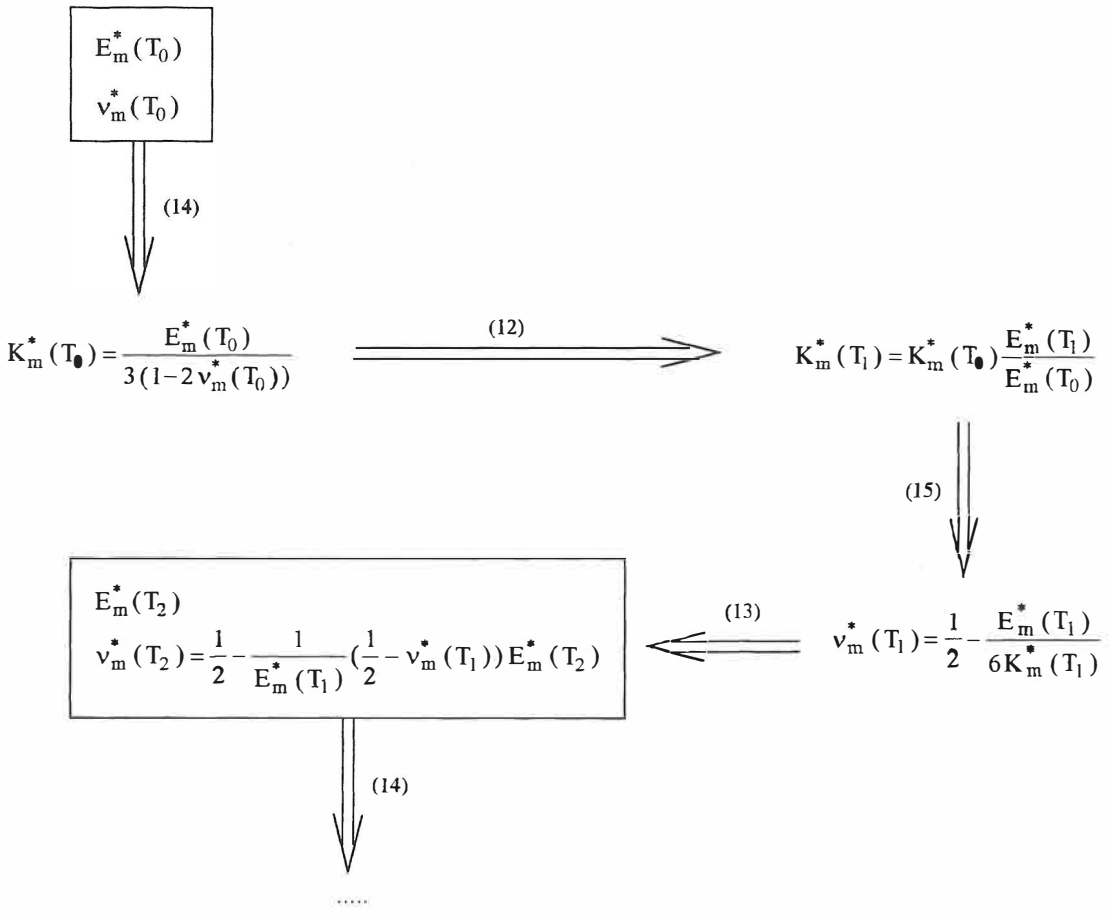

Figure 5. First step ($j = 0$) of the iterative calculus of the Poisson's ratio based on Theocaris' hypothesis.

variations with lower values for Theocaris'model. The inflexion point of ν' and the maximum of ν'' correspond to the glass transition. These tendencies were already observed on polyepoxide resins [29].

The most suitable model should be that which gives the best agreement between experimental and theoretical data. As shown on Fig. 7, the best prediction was observed with Kolsky's approach, especially on $\tan\delta$.

4.3.2. Numerical results. Two assumptions were proposed for Maurer's model:

(i) the matrix and the interphase Poisson's ratios are equal

$$\nu_i^*(T) = \nu_m^*(T), \tag{16}$$

(ii) the interphase modulus is proportional to the matrix one

$$E_i^*(T) = \alpha E_m^*(T). \tag{17}$$

Two relevant volume fractions of interphase were chosen (0.01 and 0.05%). The proportionality factor α was determined by minimizing differences on E' and E''

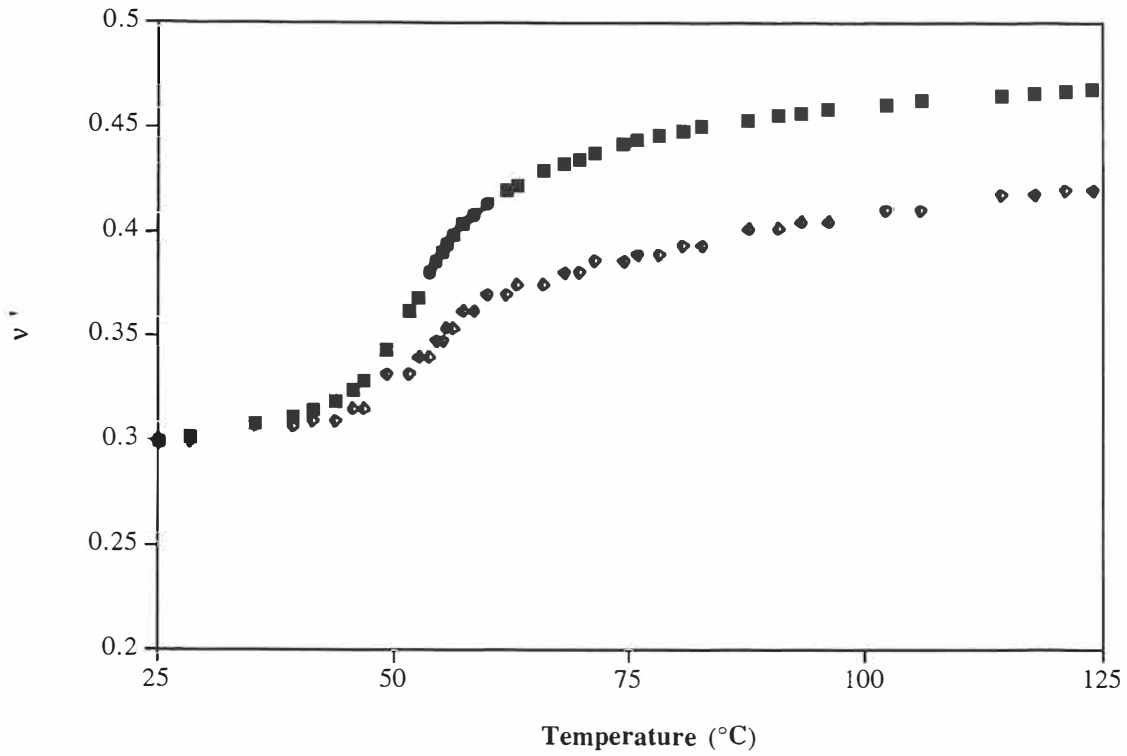

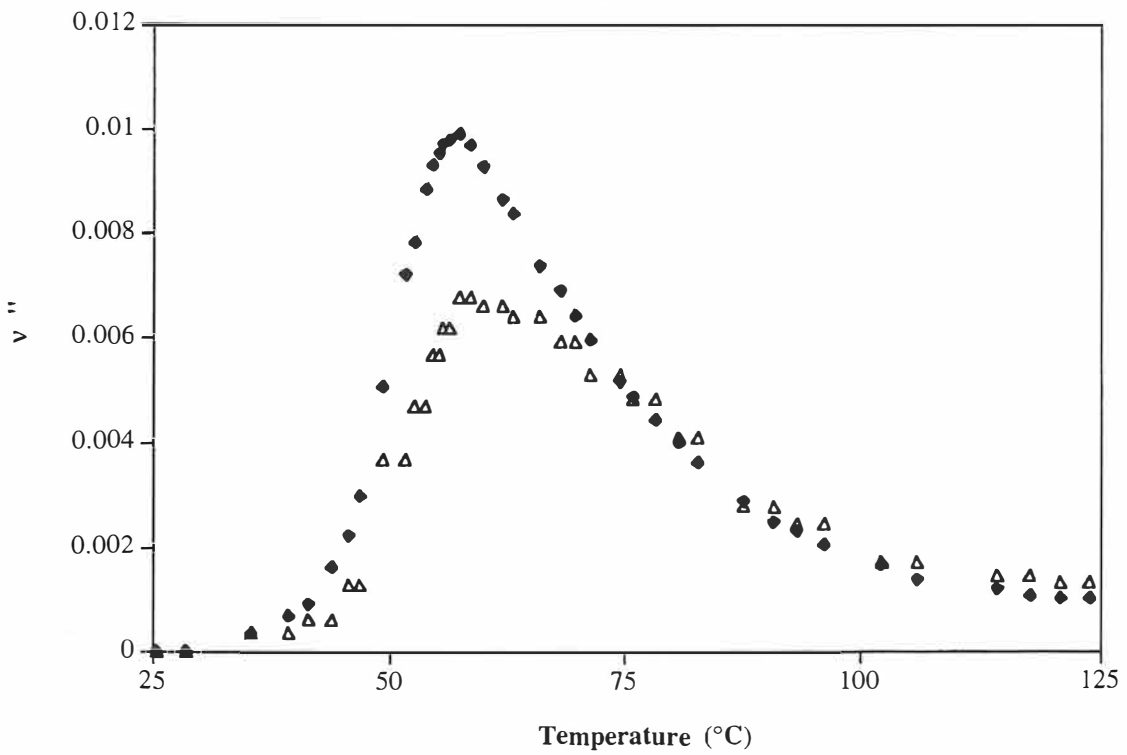

Figure 6. Theoretical curves of Poisson's ratio *versus* temperature for a poly(butylene terephthalate) matrix: Kolsky's (■) ν', (◆) ν'' and Theocaris' (◇) ν', (△) ν'' approaches.

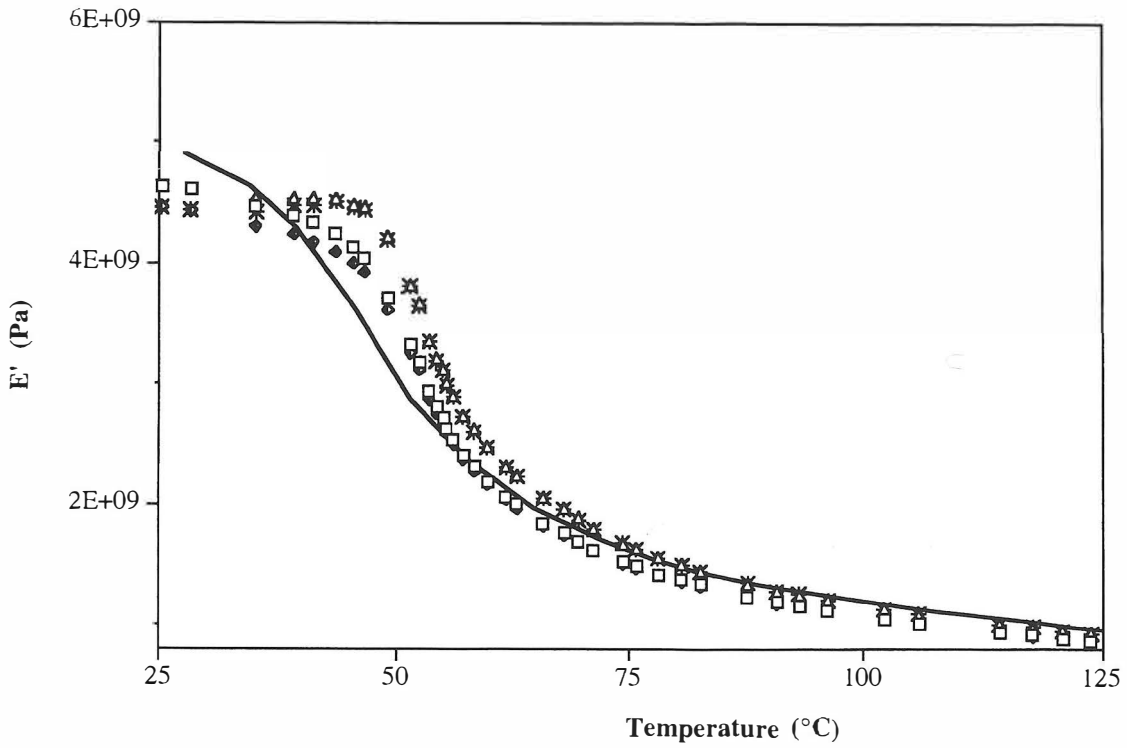

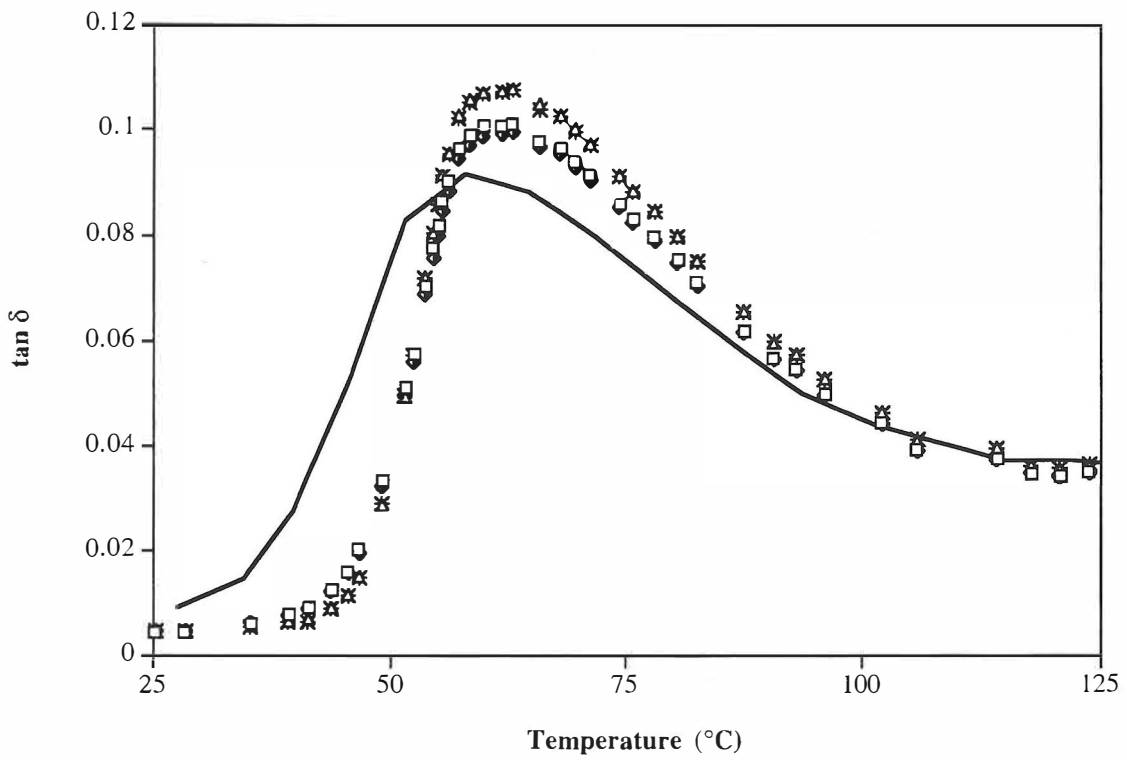

Figure 7. Choice of the prediction method of the matrix Poisson's ratio: Christensen's model (Kolsky (□), Theocaris (△)) and Maurer's model (V_i = 0.01%/Kolsky (◑), Theocaris (∗)) compared to experimental data (—) obtained for 40 wt% of aminosilane treated glass beads.

between experimental and theoretical data (average diameter 20 μm). The results are reported in Table 4.

As shown in Figs 8 and 9, the following results can be observed:

(i) slightly better predictions were obtained by taking into account the interphase properties;

(ii) whatever the surface treatment of the glass beads, the simulation seemed to be better above the temperature corresponding to the maximum of the α relaxation (T_α);

(iii) in the glassy state, the volume fraction of the interphase (V_i) seemed to have a more significant influence on E' and $\tan\delta$ data obtained by Maurer's model;

(iv) a good prediction of the magnitude of $\tan\delta$ was observed on untreated glass beads reinforced PBT.

These results showed that our numerical approaches have taken into account only the stiffness variation effect (mechanical coupling) due to matrix substitution by a more rigid phase on the one hand, and a soft layer of interphase on the other. Molecular mobility of polymer chains in the neighbourhood of the filler surface, attributed mainly to surface treatment effects and filler size distribution, did not arise in the assumptions of these models.

Previous studies [9] have already provided evidence of these two effects on viscoelastic behaviour in the case of glass beads reinforced polystyrene and acid functionalized polystyrene. For experimental results on a PBT matrix described earlier, both stiffness variation and surface treatment effects might occur.

Moreover, two additional assumptions were not taken into consideration in the self-consistent models: (i) for high filler ratios, agglomerate formation could induce sporadic phase inversion [30]; (ii) for very low ratios, the crystallinity might be of importance in the viscoelastic behaviour description.

For all these reasons, it seems very difficult to give a convincing physical interpretation to the values of the α coefficient.

Table 4.
Values obtained for α factor for two volume fractions of interphase (0.01% and 0.05%) for PBT reinforced by 40 wt% of glass beads (average diameter 20 μm) treated by vinylsilane and aminosilane coupling agents

Surface treatment	0.01%	0.05%
Vinylsilane (VS)	0.45	1.02
Aminosilane (AS)	0.21	0.35

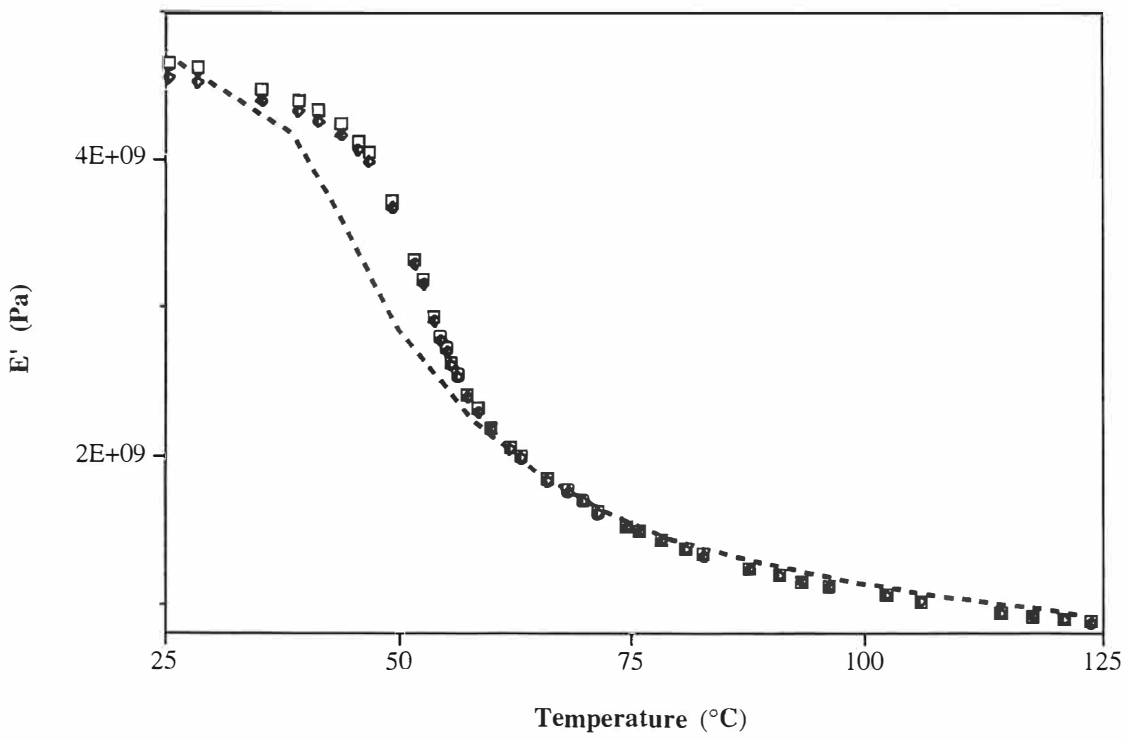

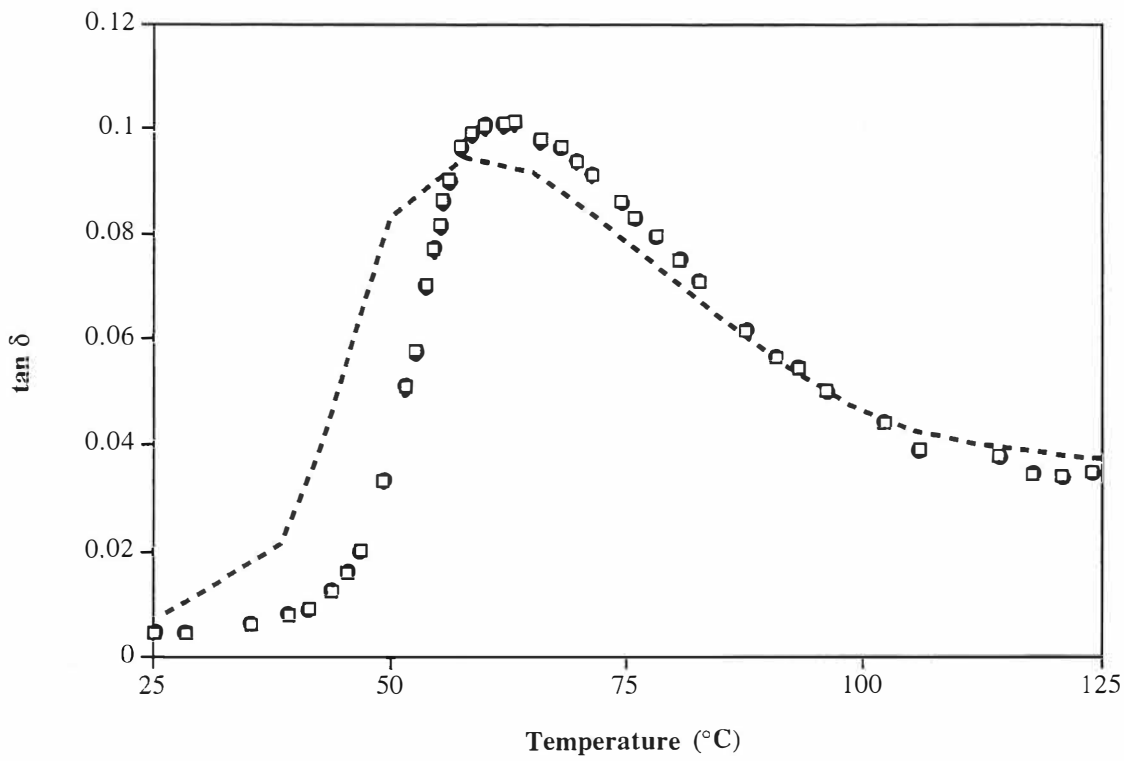

Figure 8. Theoretical curves based on the self-consistent models of (◆,○) Maurer and (□) Christensen. Comparison with a poly(butylene terephthalate) reinforced by (- - -) 40 wt% of vinylsilane treated glass beads. (Volume fraction of interphase (◆) 0.01% and (○) 0.05%.)

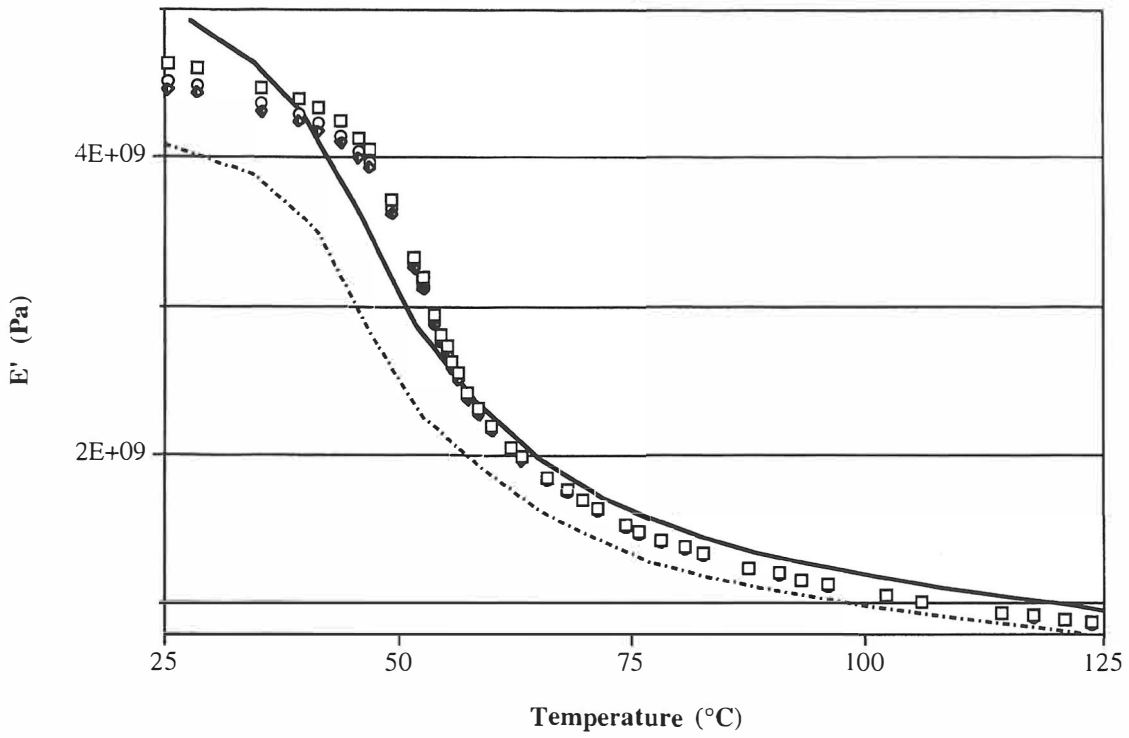

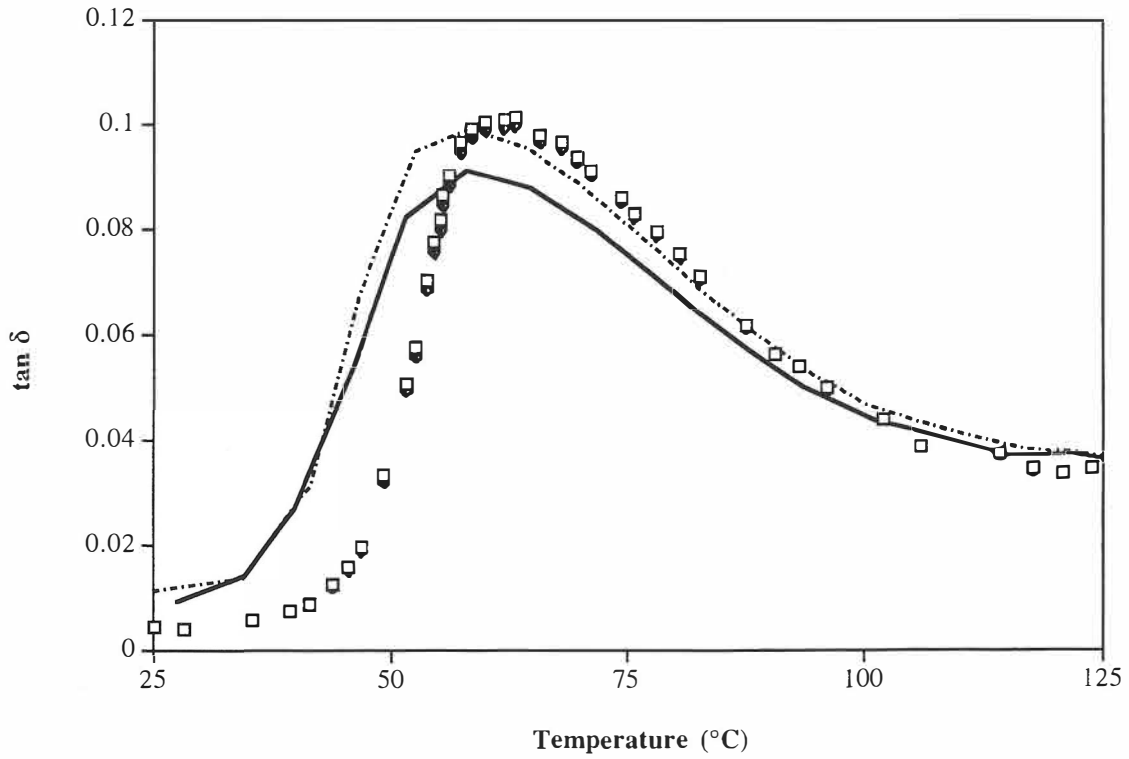

Figure 9. Theoretical curves based on the self-consistent models of (◗,○) Maurer and (□) Christensen. Comparison with a poly(butylene terephthalate) reinforced by (—) 40 wt% of aminosilane treated glass beads (volume fraction of interphase (◗) 0.01% and (○) 0.05%) and (- - -) 40 wt% of untreated glass beads.

5. CONCLUSIONS

This work has shown the value of dynamic mechanical spectrometry for the study of interfacial area in semicrystalline thermoplastics reinforced with spherical particles.

Furthermore, an approach by self-consistent models may well simulate the mechanical behaviour of these composites, but the mechanical predictions might be improved by certain additional considerations, such as:

(i) the distinction between mechanical coupling and molecular mobility of the polymer chains in the neighbourhood of the filler surface;

(ii) taking filler agglomerates into consideration;

(iii) taking cristallinity effects into account, especially for very low glass beads ratios.

REFERENCES

1. G. C. Richardson and J. A. Sauer, *Polym. Eng. Sci.* **16** (4), 252 (1976).
2. G. Landon, G. Lewis and G. F. Boden, *J. Mater. Sci.* **12**, 1605 (1977).
3. D. He and B. Z. Jiang, *J. Appl. Polym. Sci.* **49**, 617 (1993).
4. F. C. Wong and A. Ait-Kadi, *J. Appl. Polym. Sci.* **55**, 263 (1995).
5. K. P. McAlea and G. J. Besio, *Composites* **5**, 44 (1988).
6. A. Hampe, I. Boro and K. Schumacher, *Composites* **3**, 230 (1989).
7. C. Y· Yue and W. L. Cheung, *J. Mater. Sci.* **27**, 3173 (1992).
8. M. Narkis and E. J. H. Chen, *Polym. Compos.* **9** (4), 245 (1988).
9. A. Bergeret and N. Alberola, *Polymer* **37** (13), 2759 (1996).
10. M. Amdouni, H. Sautereau and J.-F. Gerard, *J· Appl. Polym. Sci.* **45**, 1799 (1992).
11. Z. V· I. Hashin, *J. Appl. Mech.* **32**, 630 (1965).
12. D. W. Woods, *Nature* **174** (4433), 753 (1954).
13. K. H. Illers and H. Breuer, *J. Coll. Sci.* **18**, 1 (1963).
14. C. Rauwendaal, in: *Polymer Extrusion*, pp. 204–219. Hanser, Munich (1990).
15. H. Katz and J. V. Milewski, in: *Handbook of Fillers for Plastics*, p. 415. Van Nostrand Reinhold, New York (1987).
16. C. D. Armeniades, *J. Polym. Sci.* **9**, 1345 (1971).
17. A. Einstein, *Annalen der Physik* **19**, 289 (1906).
18. M. Takayanagi, S. Vemuras and S. Minami, *J. Polym. Sci. C* **5**, 113 (1964).
19. E. H. Kerner, *Proc. Phys. Soc.* **69**, 808 (1956).
20. T. Mori and K. Tanaka, *Acta Metallurgica* **21**, 571 (1973).
21. P. S. Theocaris, *J. Mater. Sci.* **22**, 3407 (1987).
22. R. M. Christensen, *J. Mech. Phys. Solids* **27**, 315 (1979).
23. F. H. J. Maurer, in: *Composite Interfaces*, H. Ishida and J. L. Koenig (Eds), pp. 491–504. Elsevier Science, New York (1990).
24. J. D. Eshelby, *Proc. Phys. Soc.* **241**, 376 (1957).
25. H. A. Waterman, *Kolloid Z. Z. Polym.* **192**, 1 (1963).
26. R. Kono, *J. Phys. Soc. Jpn* **15**, 718 (1960).
27. H. Kolsky, *Stress Waves in Solids*. Oxford (1953).
28. P. S. Theocaris and C. Hadjijoseph, *Kolloid Z.* **202**, 133 (1965).
29. V· H. Nguyen, PhD Thesis, Univ. J. Fourier, Grenoble, France (1994).
30. F. De Larrard and R. Le Roy, *C.R. Acad. Sci. Paris* **314** (2), 1253 (1992).